JOURNAL OF GEOPHYSICAL RESEARCH, VOL. 101, NO. B8, PAGES 17,841–17,860, AUGUST 10, 1996

Geodesy using the Swedish permanent GPS network: Effects of signal scattering on estimates of relative site positions

R. T. K. Jaldehag,[1] J. M. Johansson, and B. O. Rönnäng

Onsala Space Observatory, Chalmers University of Technology, Onsala, Sweden

P. Elósegui,[2] J. L. Davis, and I. I. Shapiro

Harvard-Smithsonian Center for Astrophysics, Cambridge, Massachusetts

A. E. Niell

Haystack Observatory, Westford, Massachusetts

Abstract. This paper presents results from a study of elevation-angle-dependent systematic effects on estimates of relative site positions within the Swedish permanent Global Positioning System (GPS) network. Two months of data from 16 sites have been analyzed with three different elevation cutoff angles, namely, 10°, 15°, and 20°. We present offsets between these solutions and demonstrate that estimates of the vertical component of several baselines strongly depend on the minimum elevation angle (elevation cutoff angle) of the data analyzed. Offsets of 22.3 ± 1.6 mm in the vertical component are evident when the elevation cutoff angle is changed from 10° to 20°. We investigate these offsets and conclude that a significant part is due to differential phase errors caused by scattering from structures associated with the mounting of the antenna to the pillar and with the pillar itself. The horizontal components of baseline are less affected. We found, however, that the offsets in the horizontal components increase with baseline length. For the longest baselines (~1500 km) offsets of more than 5 mm are evident in the north component when the elevation cutoff angle is changed from 10° to 20°. These offsets are most likely due to differential phase errors caused by nonuniform antenna phase patterns; an effect that presumably increases with baseline length and which also might increase because of scattering from the pillars and the antenna mounts. We identify the scattering structure and reduce associated errors in the vertical component of baseline to a significant degree on one of the sites by using microwave-absorbing material. The results presented are of importance for those analyzing data from existing networks and for those who intend to establish permanent GPS geodetic networks.

Introduction

During the last few years, an increasing number of permanent Global Positioning System (GPS) sites has been established. Global networks of continuously operating GPS receivers formed with these sites are used for precise orbit determination and global geodesy and geodynamics, with repeatabilities of position estimates on all terrestrial scales reaching the level of the very long baseline interferometry (VLBI) and satellite laser ranging (SLR) techniques [e.g., *Dixon*, 1991; *Blewitt*, 1993]. The use of permanent local and regional networks, with maximum baseline lengths of ~50 km and ~1500 km, respectively, has also increased. The most demanding task for these, often multipurpose, networks is to monitor three-dimensional crustal motions associated with regional geophysical phenomena, such as postglacial rebound (e.g., J. M. Johansson et al., Geodynamics with the Global Positioning System: Two years of observations with a continuous network in Sweden, 1. Results, manuscript in preparation, 1996) (hereinafter referred to as Johansson et al., manuscript in preparation, 1996) or regional plate tectonics [e.g., *Blewitt et al.*, 1993;

[1]Now at Swedish National Testing and Research Institute, Borås.

[2]Now at ESA-INSA, IUE Observatory, VILSPA Satellite Tracking Station, Madrid.

Paper number 96JB01183.
0148-0227/96/96JB-01183$09.00

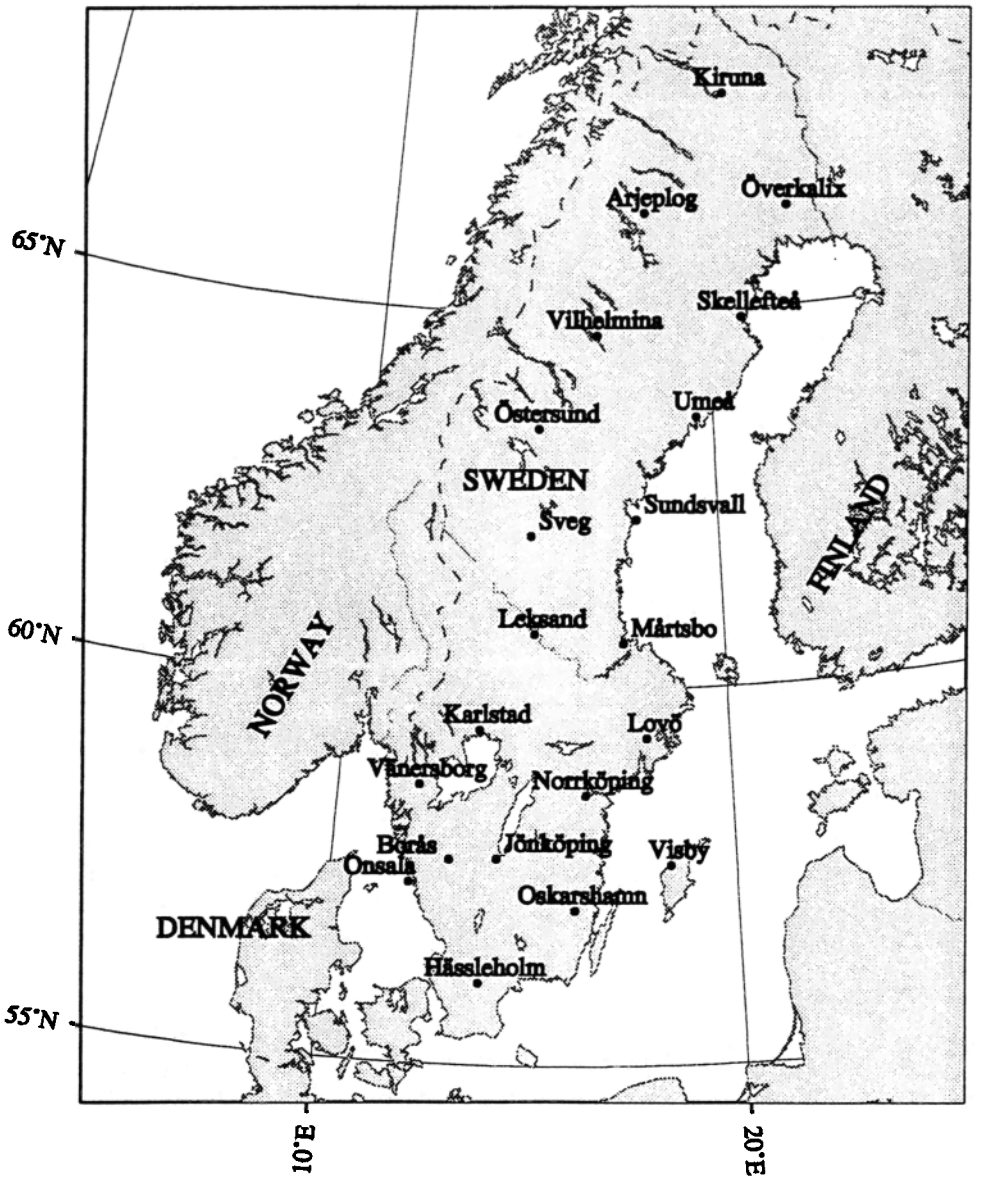

Figure 1. Geographical locations of the 20 sites of the Swedish Permanent GPS Network (SWEPOS). Those sites used in the studies of this paper are listed in Table 1.

Bock et al., 1993; *Dragert and Hyndman*, 1995; *Tsuji et al.*, 1995]. The demonstrated repeatability of horizontal position estimates for these regional networks is currently of the order of 1–2 mm and typically a factor of 3–5 greater for the vertical baseline component.

There are many advantages of continuously operating GPS networks. Stable pillars with fixed antennas eliminate errors associated with variations in the measurement of the local vector from the reference marker to the phase reference point of the antenna. For fixed pillars in a continuously operating network, the reference marker is usually a fixed, well-defined point on the antenna. Also, the cost of purchasing and maintaining equipment for a continuously operating network, averaged over a few years, is comparable to the cost of monthly or even annual field campaigns. In addition, denser position estimates (spatially and temporally) decrease the statistical uncertainty of the results. Continuously operating networks may also serve as a global or regional reference frame for different types of regional and local surveys. Another essential advantage, related to the subject of this paper, is the increased ability to study and eliminate unmodeled systematic effects on daily estimates of site positions, both short- and long-term effects.

This paper concentrates on the site-dependent error associated with the electromagnetic coupling between the antenna and its nearby environment [e.g., *Tranquilla*, 1986; *Tranquilla and Colpitts*, 1988], a study made possible thanks to the continuous operation of the Swedish permanent GPS network (SWEPOS) (Figure 1). The total electromagnetic field of an antenna

which radiates a signal in the presence of conducting structures may be expressed as a superposition of the transmitted field and the fields scattered (i.e., reflected and diffracted) by the structures. By reciprocity, the same is true for a receiving antenna. The significance of the scattered field depends on the degree of electromagnetic coupling between the antenna and the scatterer, that is, the distance to the scatterer and the size and reflectivity of the scatterer. Signal scattering affects both the amplitude and phase of the received GPS signal, presumably independently at each site in a network. This independence creates differential phase errors.

It is important to note the difference between this error and the error associated with the use of different types of antennas within the same network, even if the effects are similar. The latter error has been discussed in some detail in the literature [*Tranquilla and Colpitts*, 1988; *Schupler and Clark*, 1991; *Schupler et al.*, 1994; C. Rocken, GPS antenna mixing problems, unpublished memorandum, UNAVCO, Boulder, Colorado, 1992], showing that the use of different types of antennas within the same network, irrespective of size, necessitates phase calibration of each GPS antenna in the data analysis, if centimeter or better accuracy of vertical position estimates is required. Consequently, most GPS antennas used for geodesy and geodynamics have been phase calibrated. These calibrations have been performed, for obvious reasons, in "clean" environments such as anechoic chambers [*Schupler and Clark*, 1991; *Schupler et al.*, 1994]. However, in practice, GPS antennas are located in "dirty" environments. They are usually mounted on tripods or on concrete or metal pillars, the latter requiring stable mounts, often metallic, of the antennas. In addition, there are other types of reflecting structures in the surroundings of the antenna, such as the ground, nearby buildings, fences, etc. In the following, we assign the word "structure" to any piece of solid material that causes scattering. Scattering from surrounding structures may in fact be viewed as effectively changing the amplitude and phase characteristics of the antenna itself relative to its clean (original) pattern, that is, the antenna becomes "uncalibrated."

There are six obvious possibilities to reduce these effects (not mentioned in any specific order): (1) Measure the characteristics of the antenna with as many as possible of the structures in the vicinity of the antenna included. (2) Design the GPS antenna to be less sensitive to scattering from such structures [*Tranquilla et al.*, 1994]. It is difficult, of course, to eliminate scattering into the main lobe of the antenna, remembering that the main lobe must be sufficiently wide in order keep the gain at low elevation angles high enough. However, effects due to scattering from structures below the antenna, for example, from the ground or from structures associated with the mounting of the antenna to the pillar or with the pillar itself [*Elósegui et al.*, 1995], can be reduced by minimizing the back lobes of the antenna. Reducing the cross-polarized pattern would also help since the polarization of the GPS satellite signal, which is right-hand circular, will change upon scattering from structures. (3) Cover the structures with microwave-absorbing material thus reducing the amplitude of the scattered signals. (4) Estimate differential phase errors associated with the antenna along with other parameters using the GPS data themselves. This could, for instance, be done by modeling the phase variations with a polynomial dependent on the elevation angle. The challenge, however, would be to separate this effect from the similar dependence on elevation angle that tropospheric delays and vertical component of site position exhibit. (5) Signal processing in the receiver might also be used to reduce the effects of scattering, for example, by looking at the skewness of the signal correlation function. (6) Model the electromagnetic environment using antenna simulation software. A realistic model of the complete electromagnetic environment is difficult, if not impossible, to obtain. Nevertheless, approximate models may be useful.

Effects due to scattering from structures located many wavelengths (i.e., in the far-field range) from the antenna are often referred to as signal multipath in the literature. Signal multipath error can be assessed and modeled using geometrical ray optics as the difference between the phase of the signal arriving from the direct line-of-sight to the satellite and that of the reflected signal [e.g., *Young et al.*, 1985; *Tranquilla*, 1986; *Georgiadou and Kleusberg*, 1988]. Thus the implicit assumption when referring to multipath is that the reflecting structures are located in the far-field range of the antenna and that diffraction effects are negligible. The superposition of the direct and reflected signals, which have a common time origin at the satellite but are received out of phase, creates an interference pattern as the observed elevation angle of the satellite changes. The frequency of the interference pattern depends on the rate of change of the elevation angle, the distance to the reflecting structure, and the signal frequency. Distant reflectors create more frequent variations in the interference pattern than reflectors at closer distances. Thus, in some situations, multipath errors could be averaged out using appropriate observation times. The amplitude of the interference pattern depends not only on the area of the reflecting surface but also on the reflectivity of the reflecting structures. The original amplitude and phase characteristics of the GPS antenna can be approximately restored using the amplitude and phase of the interference pattern.

Scattering from structures located in the near-field range of the antenna (in general at distances less than a few meters for GPS antennas) is in many cases more serious than far-field scattering due to the low-frequency nature of the phase changes caused by nearby structures [*Elósegui et al.*, 1995]. Furthermore, methods using geometrical ray optics are less accurate or even unusable for determining changes in the antenna characteristics. Instead, numerical techniques, such as the method of

moments or physical optics, must be used. However, *Elósegui et al.* [1995] demonstrated that geometrical ray optics may be used to identify the scattering structure even if it is located in the near-field range of the antenna. They showed, using the multipath model discussed above, that scattering from structures located 10-20 cm below the phase reference point of the antenna, and associated with the mounting of the antenna to the pillar and with the pillar itself, produced an elevation-angle-dependent systematic error which can lead to large (centimeter or greater) errors in estimates of the vertical coordinate of site position and affects in principle all pillar-mounted antennas.

The most demanding task for SWEPOS is to measure the three-dimensional crustal motion associated with the glacial isostatic adjustment in Fennoscandia and to separate this motion from regional crustal motions of tectonic origin. The associated vertical and horizontal rates are believed to be of the order of ~0–10 mm/yr and ~0–3 mm/yr, respectively [e.g., *Mitrovica et al.*, 1994]. The existence of unmodeled systematic effects within these levels will affect our results, and possible effects must thus be investigated. We know, for instance, from the studies by *Elósegui et al.* [1995] that scattering from nearby structures around the antennas may produce systematic effects well above these levels. Errors due to scattering tend, however, to be constant from day-to-day, but any changes, temporally or spatially, associated with, for example, site environment, GPS satellite configuration, or network data analysis procedure, will also change the error and thus affect our short- and long-term results. In the following sections, we study signal scattering effects in data from SWEPOS. We document effects seen, investigate sources of error, and discuss how to reduce them. We would like to emphasize that the reported results are of general interest as similar effects are expected for most high-precision networks. In order to set the scene, we will first describe SWEPOS and the data analysis procedures used for the investigations presented in this paper.

Swedish Permanent GPS Network

SWEPOS, the Swedish permanent GPS network (Figure 1), was established in 1993 as a collaborative effort between Onsala Space Observatory, Chalmers University of Technology, Sweden, and the National Land Survey of Sweden. The use of SWEPOS for postglacial crustal rebound studies is a joint project between the Smithsonian Astrophysical Observatory, Cambridge, Massachusetts, and Onsala Space Observatory. A detailed description of SWEPOS is given by Johansson et al. (manuscript in preparation, 1996). Here we only describe some details of relevance to this paper.

SWEPOS consists of 21 sites distributed across Sweden. The minimum baseline length is ~60 km, and the maximum is ~1360 km. The maximum east-west component of baseline is ~547 km, and the maximum north-south component of baseline is ~1320 km. The average site separation is ~200 km. All sites of the network are equipped with Dorne-Margolin (DM) element antennas supplied with choke-ring ground planes and with both SNR-8000 Rogue (TurboRogue) and Ashtech Z12 receivers.

At the time of these studies, 16 sites were equipped with TurboRogue receivers (Table 1), and the results reported are based on data from these. Thirteen of these sites use ~3-m-high concrete pillars with circular cross section, on which the antennas are mounted

Table 1. Summary of Site Equipment

Site[a]	Pillar[b]	Mount[c]	Antenna
Arjeplog (ARJE)	3-m circular	Figure 2a	DM-T
Hässleholm (HASS)	3-m circular	Figure 2a	DM-T
Jönköping (JONK)	1-m circular	Figure 2a	DM-T
Karlstad (KARL)	3-m circular	Figure 2a	DM-T
Kiruna (KIRU)	3-m circular	Figure 2a	DM-T
Leksand (LEKS)	3-m circular	Figure 2a	DM-T
Mårtsbo (MART)	3-m rectangular	Figure 2a	DM-T
Onsala (ONSA)	1-m square	Figure 2b	DM-B
Östersund (OSTE)	3-m circular	Figure 2a	DM-T
Skellefteå (SKEL)	3-m circular	Figure 2a	DM-T
Sundsvall (SUND)	3-m circular	Figure 2a	DM-T
Sveg (SVEG)	3-m circular	Figure 2a	DM-T
Umeå (UMEA)	3-m circular	Figure 2a	DM-T
Vänersborg (VANE)	3-m circular	Figure 2a	DM-T
Vilhelmina (VILH)	3-m circular	Figure 2a	DM-T
Visby (VISB)	3-m circular	Figure 2a	DM-T

[a]Four-letter abbreviations for Figures 18 to 21.
[b]Height and cross section of pillar.
[c]Type of antenna mount is shown in annotated figure.

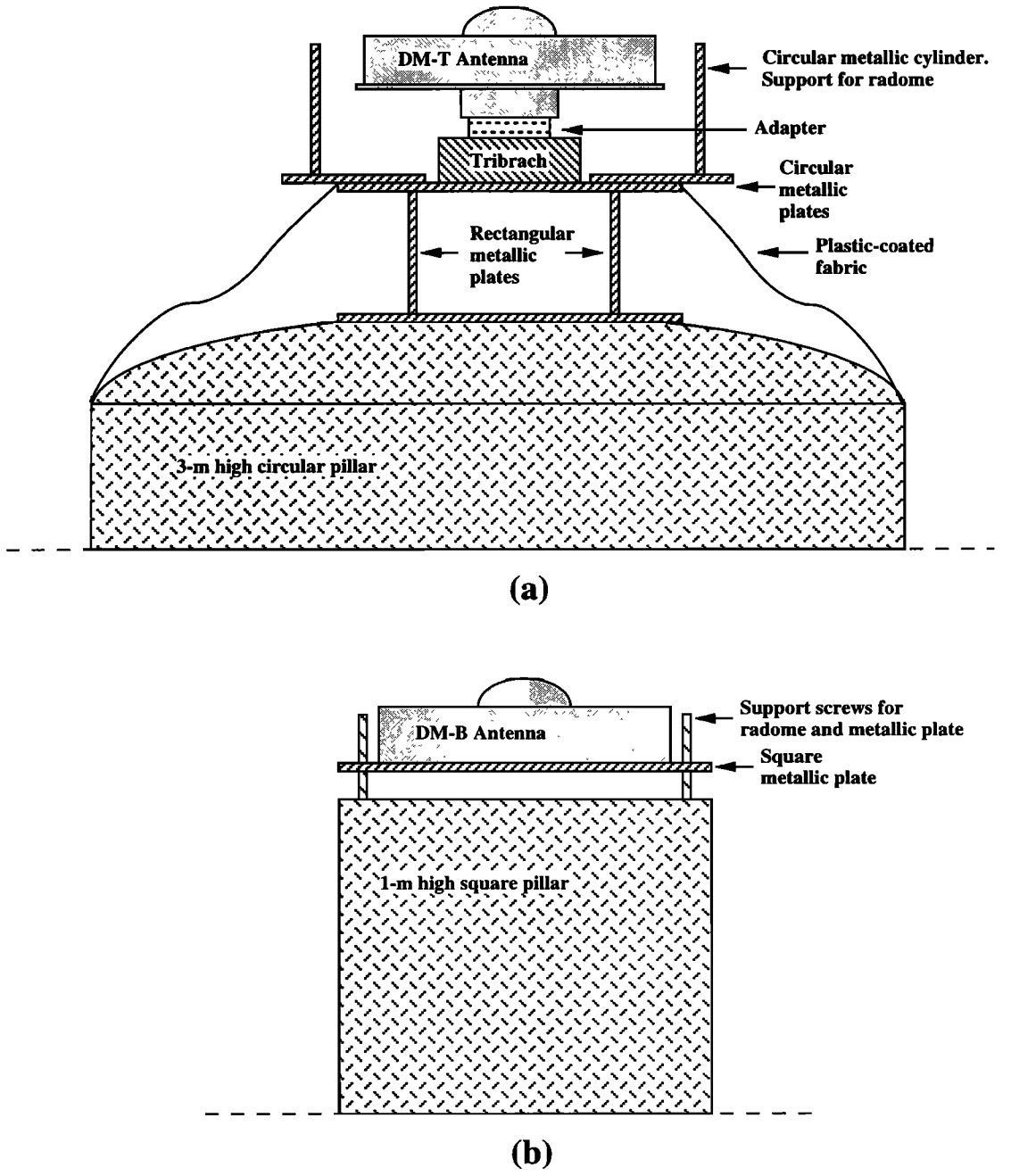

Figure 2. Sketch (drawn in scale) of the top of the pillar and the antenna mount used at (a) a major part of the SWEPOS sites and (b) the Onsala site (see also Table 1).

using identical mounting systems (Figure 2a). Of the remaining three, the Jönköping site uses an identical antenna mount and pillar, but the pillar is only ~1 m high, the Mårtsbo site has a ~3-m-high pillar but with rectangular cross section, the pillar at the Onsala site is ~1 m high with square cross section, and the antenna mount differs from that of the other 15 sites (Figure 2b). All antennas in the network are covered with conical radomes made of fiber glass in order to protect the antennas. The Onsala site uses a slightly different type of antenna (a DM type B antenna) than all the other sites in the network (which use a DM type T antenna). The amplitude and phase characteristics of these two antennas are known to be similar and are considered as identical for the studies in this paper. In the analysis below, however, this is investigated.

Analysis Procedures

Daily estimates of site positions using SWEPOS data have been obtained since August 1993 (Johansson et al., manuscript in preparation, 1996). The analysis procedure used to obtain these estimates has also been adopted for the studies in this paper. The procedure,

described in detail by Johansson et al. (manuscript in preparation, 1996), is briefly summarized here. The data are analyzed using the GIPSY-OASIS II software developed at the Jet Propulsion Laboratory [*Webb and Zumberge*, 1993, and references therein]. In addition to the SWEPOS sites, positions of nine other European sites (see Johansson et al., manuscript in preparation, 1996), equipped with Rogue-type receivers and DM antennas, are estimated in order to extend the network to the region of the glacial isostatic adjustment which is not covered by SWEPOS. Precise orbits and consistent Earth orientation parameters, produced by the International GPS Service for geodynamics (IGS), are used and not further estimated. The data sampling interval in the receivers was 30 s. These data are decimated to one sample every 240 s in the data analysis.

The analysis is carried out without the use of fiducial sites [*Heflin et al.*, 1992]. All site positions, wet tropospheric zenith delays for each site, real valued carrier phase ambiguities, satellite clocks, and site clocks, except for one adopted as the reference clock, are estimated. Ionospheric delays are removed by taking a linear combination (LC) of the dual frequency data measurements. The no-fiducial solutions are transformed to a global reference frame (ITRF) using a subset of the sites. A slightly different analysis procedure is used when only a subset of SWEPOS sites is analyzed. In this procedure, one site position is held fixed, and the other positions are estimated.

Effects of Signal Scattering on Estimates of Relative Site Positions

Anti-Spoofing Enabled

Figures 3 and 4 show the north, east, and vertical components (relative to nominal values) of the Hässleholm-Onsala and Hässleholm-Jönköping baselines between January 1, 1994, and March 31, 1994. Each plot is divided into three groups: January 1 to January 30, January 31 to February 19, and February 26 to March 31. The estimates in the first group were obtained using an elevation cutoff angle of 15°, that is, data below 15° were eliminated in the analysis. After Anti-Spoofing (AS) was enabled on January 31, we increased the elevation cutoff angle to 20° because of the corresponding decrease in signal-to-noise ratio of the GPS observables when AS is enabled. Because of the effects we saw (see below), however, the elevation cutoff angle was returned to 15° on February 26.

In Figures 3 and 4 the mean offset, relative to the nominal value, for each group of estimates is represented by solid lines. The change in offset between adjacent groups is also given numerically in Figures 3 and 4 along with the 1-σ uncertainty of the change. In the vertical component of the Hässleholm-Onsala baseline (Figure 3c), the changes between groups are 10.3 ± 1.2 mm and 9.7 ± 1.6 mm for January 31 and February 26, respectively. The change in offset on January 31 is correlated both with the enabling of AS and with the change in elevation cutoff angle. The change in offset on February 26 indicates that the differences are associated with the change in elevation cutoff angle, and not with the enabling of AS. This was later confirmed by an analysis of the January 31 to February 26 data with an elevation cutoff angle of 15°, showing consistent estimates of the January to March data (Johansson et al., manuscript in

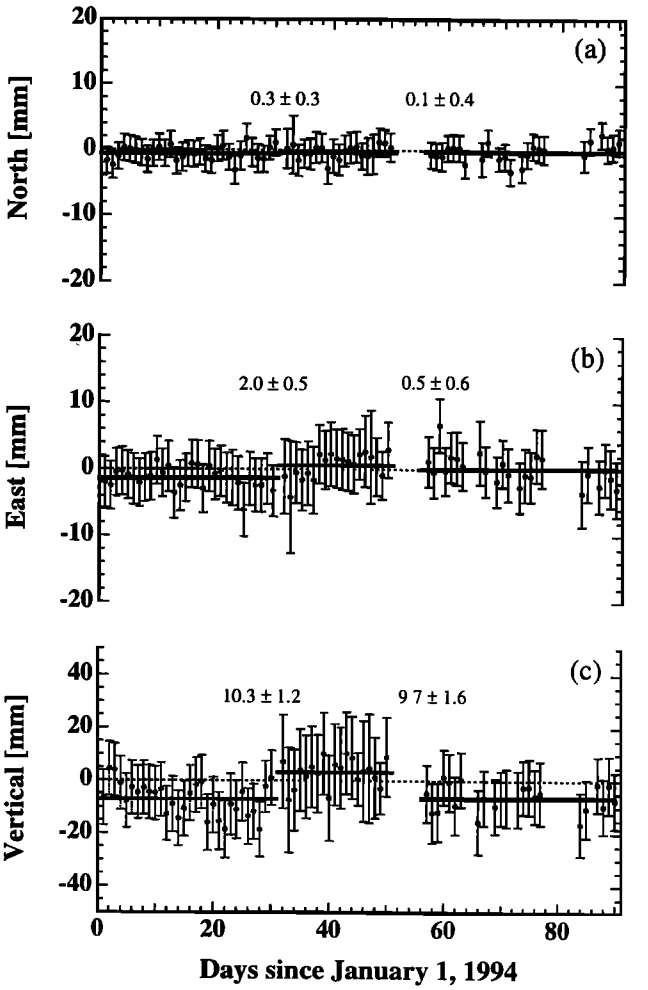

Figure 3. Daily estimates (relative nominal values) of the (a) north, (b) east, and (c) vertical components from January 1, 1994, to March 31, 1994, of the Hässleholm-Onsala baseline. The error bars are the statistical standard deviation of these estimates based on a propagated linear combination (LC) phase measurement noise of 10 mm. Each plot is divided into three groups depending on the adopted elevation cutoff angle (see text). The mean of each group of estimates is represented by solid lines. The dashed line is the zero line plotted for visual aid. The offset between two consecutive groups are given numerically along with the 1-σ uncertainty of the offset. The offsets and the uncertainty of the offsets are calculated without the use of the statistical standard deviation of the position estimates.

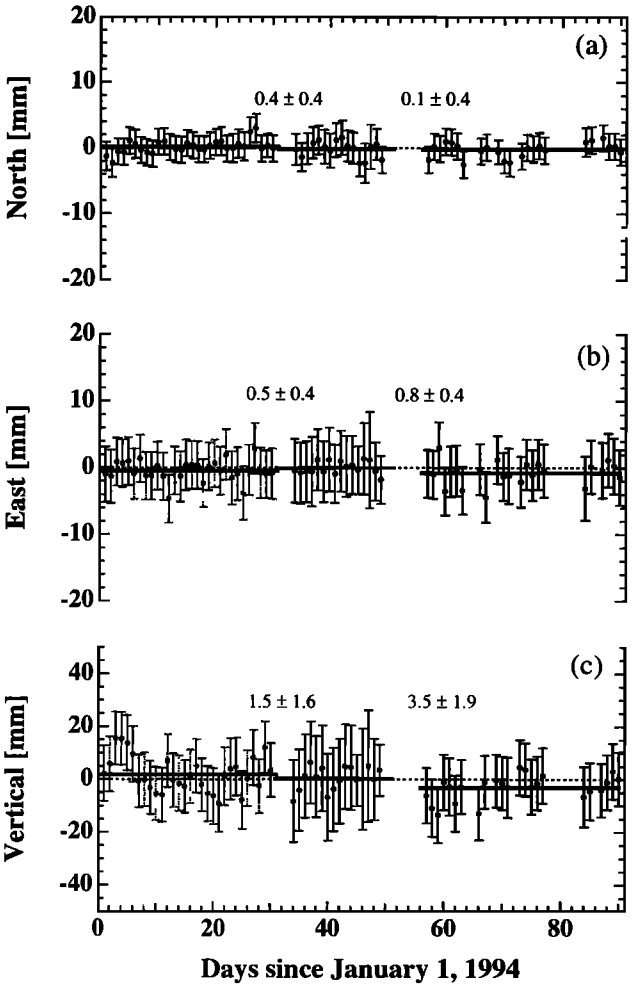

Figure 4. Same as Figure 3 except here for the Hässleholm-Jönköping baseline.

preparation, 1996). No differences are significant (3-σ) in the data of Figures 3a and 3b as well as of Figure 4, except between the first two groups in the east component of Figure 3b.

There are a few differences in equipment and monumentation between these three sites. The only difference, though, between the Hässleholm and Jönköping sites is the height of the pillars (Table 1). This difference does not seem to produce elevation-angle-dependent estimates of relative positions as seen from Figure 4. The Hässleholm and Onsala sites are less similar (Table 1): they use (1) different types of antennas and (2) different types of pillars and antenna mounts.

In order to test if the different types of antennas produce elevation-angle-dependent estimates of relative positions, we installed temporarily (24 hours) a DM-T antenna at the Onsala site. Two days of data from the Onsala site were acquired: 1 day with the DM-B antenna (July 3, 1995) and 1 day with the DM-T antenna (July 5, 1995). These data were then processed together with data collected from another TurboRogue receiver equipped with a DM-T antenna mounted on a standard wooden tripod located only ~20 m from the Onsala site pillar. The data were processed with elevation cutoff angles ranging from 15° to 50° in steps of 5°. The position of the Onsala antenna was held fixed, and no tropospheric zenith delays were estimated for this short baseline. Figure 5 shows the postfit LC phase residuals, obtained from the 15° solution on each day, for the Onsala site for all satellites from the July 3, 1995, data (Figure 5a) and from the July 5, 1995, data (Figure 5b). The qualitative similarity between Figures 5a and 5b is notable and is confirmed quantitatively in Figure 6 which shows differences in the estimated vertical component of baseline relative to the 15° solution on each day, as a function of elevation cutoff angle. It can be seen that the differences for the same elevation cutoff angle agree to less than 1 mm up to 40°.

Both Figures 5 and 6 strongly suggest that the different antenna mount and/or the pillar at the Onsala site, and not the different versions of the DM antennas, produce elevation-angle-dependent estimates of relative site positions. Evidently, differential scattering effects,

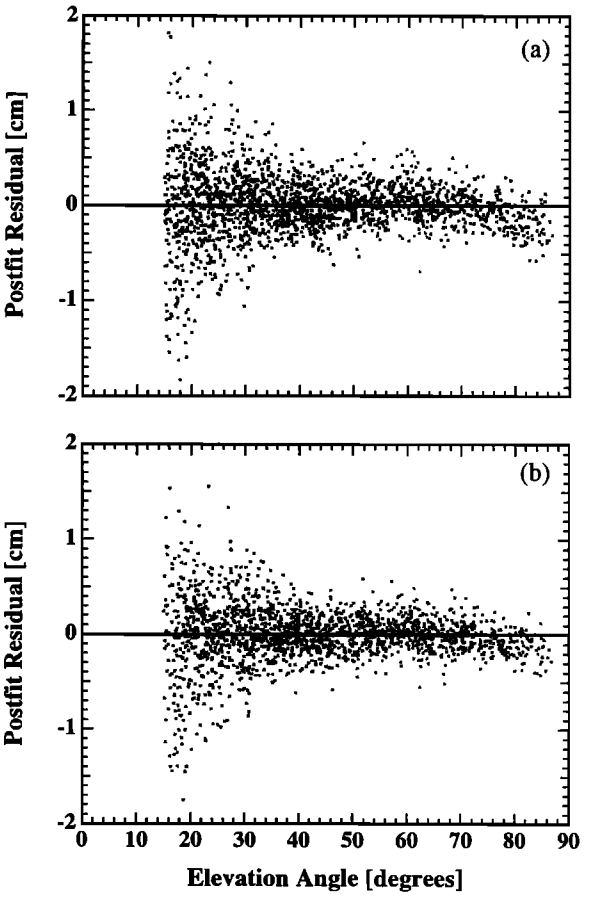

Figure 5. Postfit LC phase residuals for the Onsala site for all satellites from (a) July 3, 1994, data and (b) July 5, 1994, data, plotted as a function of elevation angle. The residuals are from the 15° solutions with (Figure 5a) a DM-B antenna and (Figure 5b) a DM-T antenna at the Onsala site's pillar.

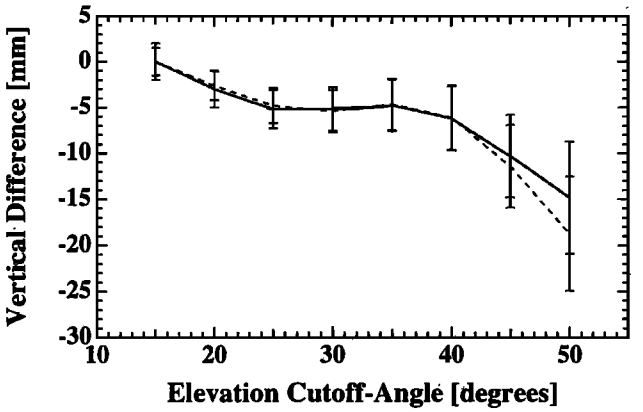

Figure 6. Differences between estimates of the vertical component of baseline as a function elevation cutoff angle. The differences are given relative to the estimate for a 15° elevation cutoff angle. The baseline is formed between the Onsala site and an antenna (DM-T) mounted on a wooden tripod located ~20 m from the Onsala site. Data are from July 3, 1994, with a DM-B antenna at the Onsala site's pillar (dashed line), and from July 5, 1994, with a DM-T antenna at the Onsala site's pillar (solid line). The error bars are the statistical standard deviation of these estimates based on a propagated LC phase measurement noise of 10 mm.

similar to those demonstrated by *Elósegui et al.* [1995], are present also within SWEPOS.

The GPS satellite orbits used in the analysis of the estimates shown in Figures 3 and 4 (and in the following) are obtained from IGS. The IGS orbits are a weighted combination of seven different orbit solutions produced by analysis centers in the United States, Canada, Germany, and Switzerland. Depending on whether or not AS is enabled, these centers may produce orbits using different elevation cutoff angles in the data analysis. The choice of elevation cutoff angle may also vary between the different centers. These differences, if existent, do not seem to affect significantly our results as seen from, for example, Figure 4c. However, in order to test this insensitivity, we produced two orbit solutions for June 16, 1994, using data from a global network of 25 sites. One orbit solution was produced by applying a 15° elevation cutoff angle to the data, and the other was produced with an elevation cutoff angle of 20°. We then used these orbits in analyses of SWEPOS data using a 15° elevation cutoff angle. We found that the difference between estimates of relative site positions from the two solutions of SWEPOS data is at the 0.1-mm level. We will not discuss this result further. The effects of using orbits obtained from an analysis using different elevation cutoff angles should, however, be investigated further, especially as the accuracy of geodetic measurements with GPS improves.

Elevation Angle Cutoff Tests

The previous section showed that estimates of relative site positions within SWEPOS depend on the choice of elevation cutoff angle. This section quantitatively assesses this effect by analyzing 1 month's worth of data (June 1994) from 16 SWEPOS sites (Table 1) using the analysis procedure described above with three different elevation cutoff angles, namely, 10°, 15°, and 20°.

Figures 7 and 8 show two examples of the time series of daily estimates in June 1994 of the north, east, and vertical components of the Hässleholm-Onsala baseline (Figure 7) and of the Hässleholm-Sundsvall baseline (Figure 8). Each plot shows estimates obtained for the three different elevation cutoff angles. In both Figures 7 and 8, we have omitted the error bars and connected consecutive estimates with lines for clarity. Clear, con-

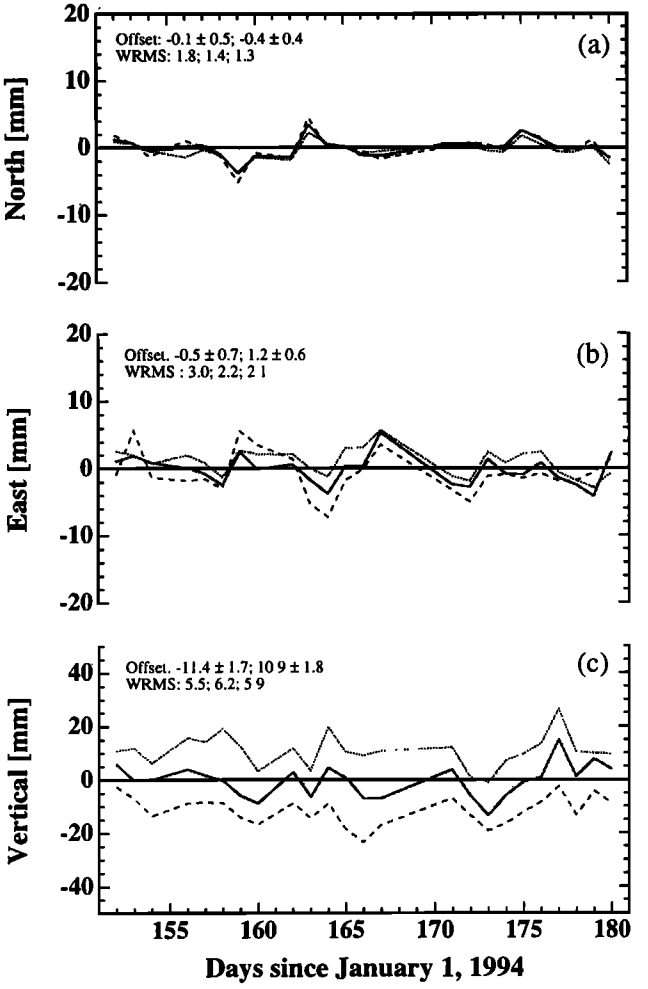

Figure 7. Daily estimates of the (a) north, (b) east, and (c) vertical components of the Hässleholm-Onsala baseline in June 1994 for three different elevation cutoff angles, namely 10° (dashed lines), 15°(solid lines), and 20° (dotted lines). The error bars, omitted for clarity, are as explained in Figure 3. They amount on average to 4.4 mm, 4.8 mm, and 5.5 mm for the 10°, 15°, and 20° solutions, respectively, for the north components, to 8.6 mm, 9.6 mm, and 11.1 mm for the east components, and to 17.4 mm, 24.3 mm, and 35.2 mm for the vertical components. The mean offsets between the 15° solutions and the 10° and 20° solutions are given in each plot (ordered 15°–10°and 15°–20°) along with weighted RMS values (ordered 10°, 15°, and 20°) of each solution (see text).

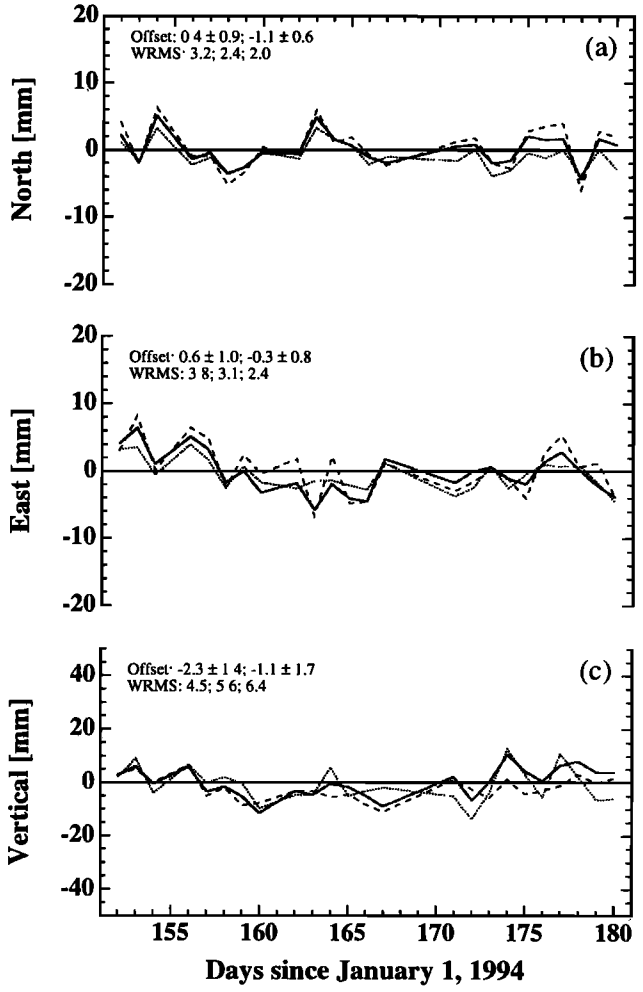

Figure 8. Same as Figure 7, except here for the Hässleholm-Sundsvall baseline. The size of the error bars are also similar to those given in Figure 7.

sistent offsets are seen in the vertical component of the Hässleholm-Onsala baseline but not of the Hässleholm-Sundsvall baseline. The monthly combined solutions (i.e., the weighted combination of 1 month of daily estimates for a specific elevation cutoff angle, referred to as the combined solution in the following) for 10° and 20° elevation cutoff angle differ by 22.3 ± 1.6 mm in the vertical component of the Onsala-Hässleholm baseline. No significant (3-σ) offsets are evident in the horizontal components of these baselines. These results are in good agreement with the results presented in the previous section.

Table 2 summarizes, for all the 16 sites, comparisons between combined solutions of daily estimates of relative positions in June 1994. Table 2 is divided into three main columns, one for each baseline component. Each column is further divided into two subcolumns. In the first subcolumn, we give the mean $\bar{D}$ of the absolute values of the offsets between the estimated baseline components for the combined solutions for 10° or 20° elevation cutoff angle and the combined solution for a 15° elevation cutoff angle. The absolute values of the offsets are given so that a negative offset (i.e., the baseline component gets shorter when changing the elevation cutoff angle) does not average out a positive offset. The uncertainties given in Table 2 are the standard deviation of the absolute values of the offsets divided by the square root of the number of baselines to the specific site. In order to separate the effects for identical versus nonidentical antenna mounts, and to some extent also the effects of different pillars, the offsets given in Table 2 for the Onsala site are based on baselines to all other sites, whereas the offsets for all other sites are based on baselines to all sites except the Onsala site.

The second subcolumn gives the ratio W_r between the mean of the weighted RMS (WRMS) of all baselines to the specific site for the 15° solution and the mean of the WRMS of all baselines to the specific site for the 10° or 20° solution. The WRMS is a measure of the repeatability of the time series. For a W_r below 1, the repeatability is worse (i.e., the WRMS is higher) for the indicated elevation cutoff angle compared to the repeatability of the 15° solution, and it is better (i.e., the WRMS is lower) for a W_r above 1. Since each row gives results for baselines from the specific site to all other sites (with the exceptions mentioned above), there is a correlation between values in each row. The last row in Table 2 gives the means for each column.

Several interesting results can be found from Table 2. The offsets in the horizontal components are of the order of 1 mm or less but are significant as seen from the standard errors shown in Table 2. The offsets are larger for a change in elevation cutoff angle from 15° to 20° than from 15° to 10°. The mean (as seen from the last row in Table 2) of the offsets in the horizontal components relative to the 15° solution is about 1 mm when a cutoff angle of 20° is applied and about 0.5 mm when a cutoff angle of 10° is applied. The mean WRMS (also seen from the last row in Table 2) of the 20° solution is about 20% lower than the corresponding mean WRMS of the 15° solution. The mean WRMS for the 10° solution is about 20% and 10% higher for the north and east components, respectively. We see also that the estimated horizontal components seem to be insensitive to the combination of antenna mount and pillar types.

The vertical component behaves differently. Offsets of about 10 mm are evident for both the 10° and 20° solutions for the Onsala site, which uses a unique type of pillar and antenna mount. For other sites, the offsets range from about 2 mm to 4 mm, with exception of the Kiruna, Mårtsbo, Östersund, Skellefteå, and Visby sites. The offsets for these sites, which range from 5 mm to 10 mm, are more difficult to explain than the offsets for the Onsala site. One similarity between these five sites, however, is that their pillars are located fairly close (~0.5– ~5 m) to the receiver cabin. At all other sites, the pillar is located more than about 5 m from the cabin (Johansson et al., manuscript in preparation, 1996). Scattering from the cabin roof may produce elevation-angle-dependent errors which would affect the baseline estimates. The mean WRMS of the

Table 2. Absolute Values of Offsets[a] Between Combined Solutions of June 1994 Data for Three Different Elevation Cutoff Angles: 10°, 15°, and 20°

Site	North				East				Vertical			
	$\bar{D}$,[b] mm		W_r[c]		$\bar{D}$, mm		W_r		$\bar{D}$, mm		W_r	
	10°	20°	10°	20°	10°	20°	10°	20°	10°	20°	10°	20°
Arjeplog	0.38 ± 0.07	0.87 ± 0.16	0.93	1.12	0.38 ± 0.09	0.97 ± 0.18	0.96	1.07	2.29 ± 0.36	4.42 ± 0.60	0.86	0.95
Hässleholm	0.67 ± 0.14	1.50 ± 0.28	0.76	1.17	0.39 ± 0.08	0.54 ± 0.11	0.83	1.12	3.16 ± 0.55	3.44 ± 0.85	1.09	0.87
Jönköping	0.53 ± 0.11	1.41 ± 0.23	0.79	1.12	0.46 ± 0.08	0.92 ± 0.16	0.86	1.17	2.49 ± 0.52	2.90 ± 0.82	0.99	0.91
Karlstad	0.35 ± 0.10	0.85 ± 0.16	0.78	1.15	0.50 ± 0.09	0.76 ± 0.12	0.88	1.10	2.83 ± 0.55	3.02 ± 0.73	0.99	0.91
Kiruna	0.76 ± 0.18	1.27 ± 0.19	0.90	1.11	0.51 ± 0.11	0.75 ± 0 16	0.99	1.29	5.40 ± 0.58	2.97 ± 0.88	0.89	0.79
Leksand	0.31 ± 0.05	0.74 ± 0.15	0.83	1.18	0.92 ± 0.12	1.09 ± 0.16	0.92	1.28	3.24 ± 0.52	4.42 ± 0.58	0.95	0.87
Mårtsbo	0.33 ± 0.04	0.68 ± 0.11	0.79	1.19	0.51 ± 0.08	0.56 ± 0.12	0.91	1.17	6.23 ± 0 57	2.99 ± 0.64	1.05	0.89
Onsala	0.36 ± 0.07	0.80 ± 0.21	0.80	1.17	0.61 ± 0.10	1.15 ± 0.16	0.88	1.16	9.20 ± 0.68	13.65 ± 0.93	1.06	0.99
Östersund	0.36 ± 0.07	0.85 ± 0.22	0.81	1 21	0.41 ± 0.08	0.61 ± 0.13	0.89	1.32	2.12 ± 0.47	5.70 ± 0.65	1.04	0.80
Skellefteå	0.30 ± 0 04	1.08 ± 0.26	0.81	1.04	0.40 ± 0.09	0.69 ± 0.12	0.93	1.19	2.02 ± 0.48	10.17 ± 0.77	1.11	0.89
Sundsvall	0.34 ± 0.06	0.72 ± 0.13	0.81	1.28	0.66 ± 0.12	0.67 ± 0.13	0.87	1.40	2.18 ± 0.47	3.06 ± 0.91	1.09	0.87
Sveg	0.42 ± 0.08	0.68 ± 0.15	0.77	1.22	0.74 ± 0.12	0.55 ± 0.10	0.85	1.12	2.01 ± 0.44	4.36 ± 0.94	0.96	0.82
Umeå	0.27 ± 0.06	0.66 ± 0.10	0.81	1.27	0.38 ± 0.09	0.78 ± 0.12	0.94	1.32	2.61 ± 0.52	3.51 ± 0.94	1.08	0.86
Vänersborg	0.38 ± 0.07	0.98 ± 0.15	0.85	1.22	0.44 ± 0.09	0.91 ± 0 13	0 85	1.07	4.02 ± 0.61	3.61 ± 0.49	0.96	0.93
Vilhelmina	0.30 ± 0.05	0.69 ± 0.18	0.84	1 24	0.97 ± 0.10	1.29 ± 0.15	1.00	1.20	2.03 ± 0.43	2.95 ± 0.69	0.97	0.79
Visby	0.54 ± 0.08	0.56 ± 0.09	0.76	1.07	0.73 ± 0.15	1.02 ± 0.18	0.90	1.21	4.25 ± 0.61	6.61 ± 1.01	0.95	0.84
Mean	0.41 ± 0.08	0.90 ± 0.17	0.81	1.17	0.56 ± 0.10	0.83 ± 0.14	0.90	1.20	3.51 ± 0.52	4.86 ± 0.78	1.00	0.87

[a]The offsets are relative to the 15° solution

[b]The mean of the absolute values of the offsets. The uncertainty is the standard error of the mean.

[c]Ratio between the mean of the weighted RMS of all baselines to the specific site for the 15° solution and the mean of the weighted RMS of all baselines to the specific site for the 10° or 20° solution.

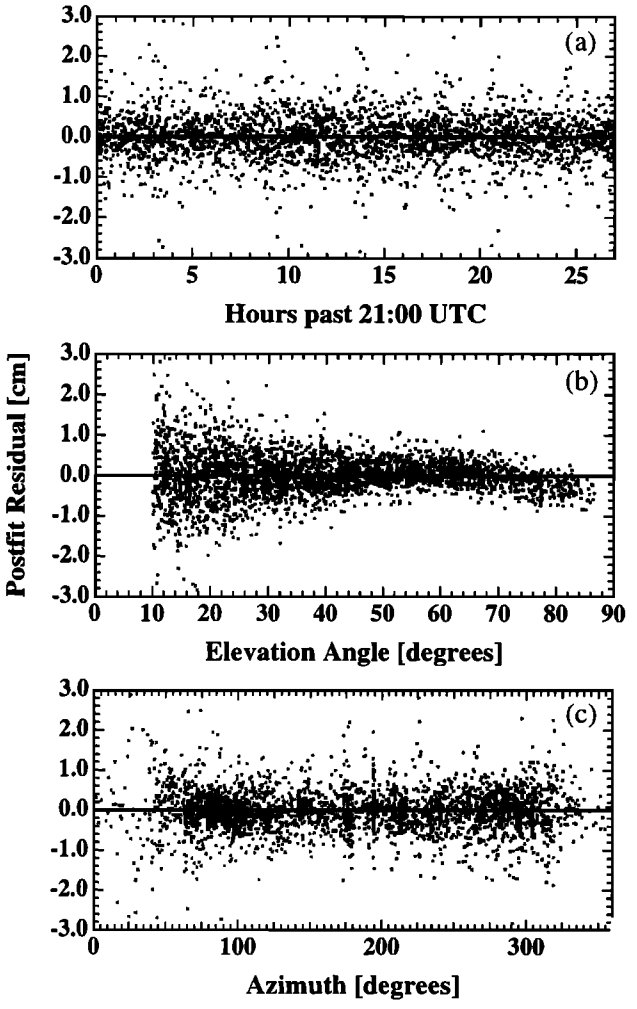

Figure 9. Postfit LC phase residuals for the Onsala site for all satellites from the June 16, 1994, data, plotted as a function of (a) time, (b) elevation angle, and (c) azimuth.

vertical component of the 15° solution is about 10–15% lower than the corresponding mean WRMS of the 20° solution, and similar to that of the 10° solution, but varies between 0.89 for the Kiruna site to 1.11 for the Skellefteå site.

The elevation-angle-dependent offsets related to the Onsala site can also be understood by a look at postfit residuals. Figure 9 shows postfit LC phase residuals for the Onsala site for all satellites from the June 16, 1994, data, plotted as a function of (Figure 9a) time, (Figure 9b) elevation angle, and (Figure 9c) azimuth. The fact that systematic variations can be seen only when the residuals are plotted as a function of elevation angle indicates that the offsets are mainly elevation-angle-dependent. As mentioned in the introduction, the frequency of the variations in, for example, postfit residuals, is dependent on the distance to the scattering structures. The slowly varying postfit residuals of the Onsala site shown in Figure 9b indicate that the scattering structures are located within a wavelength ($\lesssim$20 cm) beneath the phase reference point of the antenna [*Elósegui et al.*, 1995], that is, associated with the top of the pillar and/or the antenna mount. One way to test this is to cover with microwave-absorbing material the top of the pillar and the structures associated with the antenna mount. Results from such a test will be given in the next section.

First, however, we may draw three main conclusions from the results presented in this section: (1) Unmodeled elevation-angle-dependent systematic effects, related to the pillar systems and the distance between the antenna and the receiver cabin, may affect the accuracy of the parameters estimated. The precision, on the other hand, or estimates of rates of baseline changes, do not have to be affected as effects due to scattering tend to be constant from day-to-day. However, any changes in the site equipment or in the analysis procedure, as discussed in the introduction, may affect the precision of the order of several centimeters. (2) On average, we do not gain very much in terms of repeatability in the vertical component by choosing a 10° elevation cutoff angle instead of a 15° elevation cutoff angle. At the same time, the repeatabilities in the horizontal components deteriorate by about 10-20%. (3) The repeatabilities in the horizontal components are about 20% better with a choice of 20° elevation cutoff angle compared to the 15° solution, but at the same time, the repeatability in the vertical component deteriorates by about 10%. The last two conclusions imply that a choice of 15° elevation cutoff angle seems to be best overall in terms of repeatability for processing SWEPOS data, at least when AS is enabled and with the current choice of receiver/antenna equipment.

Test With Microwave Absorber

As mentioned in the introduction, one way to possibly reduce signal scattering effects is to cover the scatterer with microwave-absorbing material. On August 10, 1994, we placed a square piece (61×61×5.7 cm) of microwave-absorbing material (Eccosorb AN-W with a reflectivity of less than -18 dB above 1 GHz) in between the rectangular metallic plate on which the antenna is mounted and the top of the pillar (Figure 2b). On August 23, 1994, we moved the absorber to a place just above the rectangular metallic plate. Postfit LC phase residuals for the Onsala site for all satellites from August 11, 1994, data (the microwave absorber below the metallic plate) and from September 16, 1994, data (the microwave absorber just above the metallic plate) are plotted as a function of elevation angle in Figures 10a and 10b, respectively. The systematic variations with elevation angle are significantly reduced with the absorber just above the metallic plate (Figure 10b) but are still significant (compare with Figure 9b) with the absorber below the metallic plate (Figure 10a). This result indicates that the metallic plate is the main scatterer.

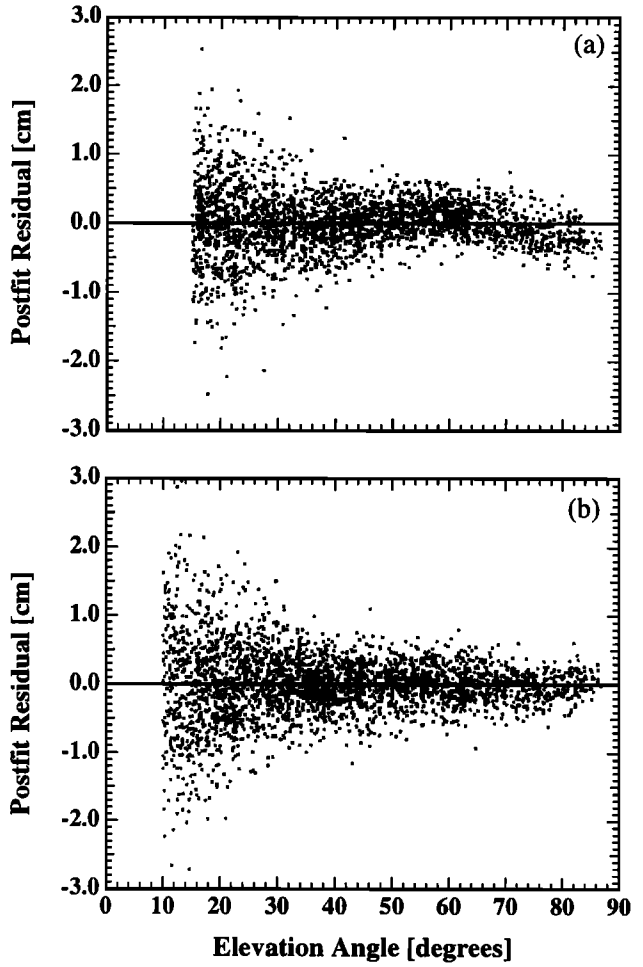

Figure 10. Postfit LC phase residuals for the Onsala site for all satellites from the (a) August 11, 1994, data and (b) September 16, 1994, data, plotted as a function of elevation angle. Microwave absorber at the Onsala site located (Figure 10a) in between the pillar and the metallic plate and (Figure 10b) just above the metallic plate (Figure 2b).

Figures 11 and 12 show time series of daily estimates in September 1994 (i.e., with the microwave absorber just above the metallic plate at the Onsala site) of the north, east, and vertical components of the same baselines as in Figures 7 and 8, respectively. We see that the offsets in the vertical component between the three solutions for 10°, 15°, and 20° elevation cutoff angle have been reduced for the Hässleholm-Onsala baseline compared to those in Figure 7c. The offset in the vertical component between the combined solutions for 10° and 20° elevation cutoff angles is reduced by more than 60%, to 7.8 ± 1.4 mm. The offsets for the Hässleholm-Sundsvall baseline, and for the horizontal components of both baselines, are about the same as in Figures 7 and 8 and within the 3-σ uncertainties.

Table 3 summarizes comparisons between combined solutions of daily estimates of positions in September 1994. A comparison of the results of the horizontal components with those in June reveals no significan changes. If we compare the results of the vertical component with those in June, we see that the offsets for the Onsala site have been reduced as also indicated in Figure 11c. The offset for the 10° solution has been reduced by about 30% and for the 20° solution by about 60%. If we compare results for other sites, we see that the relatively large offsets for the Östersund, Skellefteå, and Visby sites are still apparent. A few discrepancies can also be seen. An offset of 5.9 mm for the Karlstad site for the 20° solution is now apparent. The reason for this offset, however, is known to be due to a malfunction in the receiver at this site in September. What is more confusing, though, is that the large offsets for the Kiruna and Mårtsbo sites for the 10° solution for the June data, are not apparent in the corresponding solution for the September data. One reason might be, as mentioned above, that the pillars at these sites are located fairly close to the receiver cabins which might cause variations in the scattering effects, but there might also be other reasons for this discrepancy, as of now of unknown character.

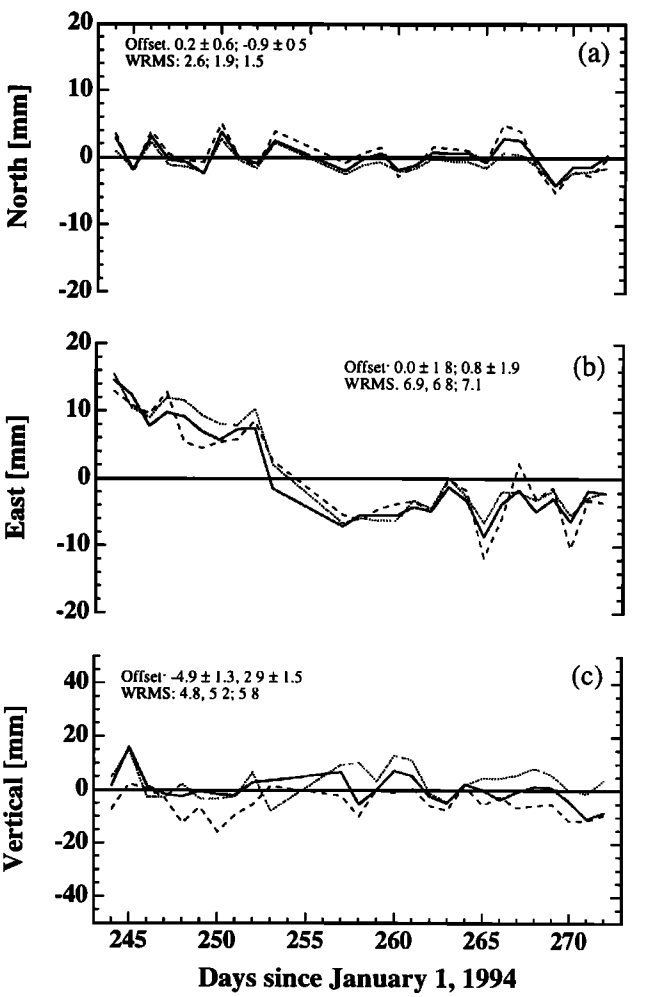

Figure 11. Same as Figure 7, except here for September 1994.

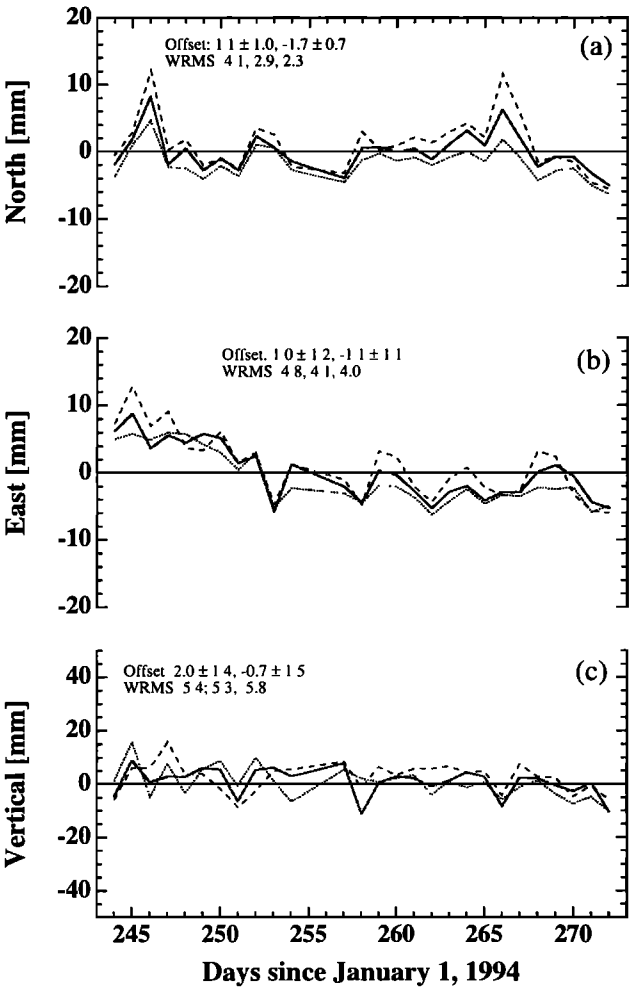

Figure 12. Same as Figure 8, except here for September 1994.

The WRMS ratios W_r of the horizontal components are similar to those in June, that is, the repeatabilities are improved for a 20° elevation cutoff angle and deteriorated for a 10° elevation cutoff angle, both compared to the solution for a 15° elevation cutoff angle. The mean WRMS ratio of the vertical component is similar to that in June for the 20° solution but somewhat higher for the 10° solution. The average improvement for the 10° solution is difficult to explain. In principle, we should not expect big differences for other sites than Onsala, in any component. The changes we see might be due to what we have discussed above; otherwise, the changes must be random and due to the fact that we have analyzed 2 different months. One of the changes that is statistically certain, though, is the decreased offsets for the Onsala site, as also indicated from the postfit LC phase residuals for the Onsala site on September 16 (Figure 10b). Unmodeled systematic effects for one site may also affect estimates of positions at other sites because of estimates of parameters which are common to different sites. The fact that unmodeled elevation-angle-dependent systematic effects for the Onsala site have been reduced might explain the small improvements at the other sites as well.

In order to study the effects of the microwave absorber on estimates of the vertical component of baseline over a wider range of elevation cutoff angles, three baselines within SWEPOS were processed separately with elevation cutoff angles adjusted from 5° to 50° in steps of 5°. About 6 weeks' worth of data was analyzed, 3 weeks (August 1–22, 1994) before and 3 weeks (August 23–September 16, 1994) after the inclusion of the microwave absorber at the Onsala site. Combined solutions were then formed for each elevation cutoff angle and for each 3-week period. The first period includes the days when the absorber was located below the metallic plate.

Figure 13 shows variations in the vertical component of baseline as a function of elevation cutoff angle of the (Figure 13a) Hässleholm-Onsala, (Figure 13b) Onsala-Sundsvall, and (Figure 13c) Hässleholm-Sundsvall baselines (no microwave absorber is involved in the Hässleholm-Sundsvall baseline since the baselines are processed separately). The results are shown relative to the combined 5° solution of the first 3-week period. It is seen that the variations in the vertical component of the baselines including the Onsala site are significantly reduced when the microwave absorber is in place above the plate. The variations in the Hässleholm-Sundsvall baseline display a nonsystematic behavior in both periods. This might, however, be an effect of the degree of cancellation of common scattering effects.

Remaining unmodeled systematic effects in, for example, Figures 13a and 13b or in Table 3 for the Onsala site, indicate either the presence of possible scattering effects at other sites in the network or remaining scattering effects at the Onsala site. The purpose of the absorber was to identify the scatterer and reduce its effect on estimates of relative site positions, and the results reported certainly indicate both. Nothing implies, though, that the scattering effects at the Onsala site with the absorber employed should be identical to the scattering effects at the other sites in the network, even if the difference seems to be smaller.

What about variations in postfit residuals for other sites of SWEPOS and of the additional European sites used in the analysis? Figure 14 shows postfit LC phase residuals for the Hässleholm site (Figure 14a) and for the Kootwijk site in the Netherlands (Figure 14b) for all satellites from September 16, 1994, data. The baseline length from Kootwijk to the closest SWEPOS site (Hässleholm) is only ~675 km. Kootwijk is also one of the sites used to transform the no-fiducial solution to the ITRF (see above). The residuals for the Hässleholm site display no elevation-angle-dependence, whereas the residuals for the Kootwijk site display an elevation-angle-dependence similar to that of the Onsala site on June 16, 1994 (Figure 9b).

The combined solutions of daily estimates of the vertical component in June and September 1994 of the

Table 3. Absolute Values of Offsets[a] Between Combined Solutions of September 1994 Data for Three Different Elevation Cutoff Angles: 10°, 15°, and 20°

Site	North				East				Vertical			
	$\tilde{D}$,[b] mm		W_r[c]		$\tilde{D}$, mm		W_r		$\tilde{D}$, mm		W_r	
	10°	20°	10°	20°	10°	20°	10°	20°	10°	20°	10°	20°
Arjeplog	0.41 ± 0.12	1.04 ± 0.20	0.81	1.15	0.61 ± 0.15	1 22 ± 0.20	0.71	1.03	2.58 ± 0.57	4.41 ± 0.77	1.14	0.86
Hässleholm	1.12 ± 0.15	2.07 ± 0.30	0.73	1.24	0.61 ± 0.09	0.61 ± 0.14	0.83	1.06	2.33 ± 0.49	3.34 ± 0.62	1.10	0.96
Jönköping	0.57 ± 0.13	1.63 ± 0.27	0.75	1.16	0.42 ± 0.08	0.61 ± 0.13	0.78	1.24	2.48 ± 0.59	2.45 ± 0.58	1.08	0.97
Karlstad	0.45 ± 0.08	0.84 ± 0.19	0.75	1.24	0.41 ± 0.07	0.85 ± 0.14	0.82	1.03	2.92 ± 0.61	6.09 ± 0.69	1.10	0.92
Kiruna	0.93 ± 0.19	1.58 ± 0.27	0.80	1.13	0.60 ± 0.14	1.11 ± 0.19	0.79	1.08	3.10 ± 0.49	2.82 ± 0.55	1.22	0.90
Leksand	0.79 ± 0.13	0.97 ± 0.20	0.75	1.23	1.02 ± 0.13	1.56 ± 0.17	0.75	1.07	4.28 ± 0.56	3.95 ± 0.65	1.07	0.77
Mårtsbo	0.48 ± 0.09	0.83 ± 0.17	0.79	1.25	0.52 ± 0.12	0.68 ± 0.12	0.71	1.16	2.35 ± 0.49	2.57 ± 0.58	0.96	0.98
Onsala	0.49 ± 0.11	1.09 ± 0.20	0.85	1.15	0.63 ± 0.08	1.11 ± 0.16	0.92	0.95	6.52 ± 0.60	5.15 ± 0.71	1.02	0.81
Östersund	0.52 ± 0.12	0.91 ± 0.20	0.74	1.15	0.47 ± 0.10	0.84 ± 0.15	0.86	1.13	2.13 ± 0.28	5.01 ± 0.79	0.89	0.83
Skellefteå	0.47 ± 0.11	1.02 ± 0.27	0.75	1.12	0.43 ± 0.11	0.93 ± 0.14	0.81	1.15	2.38 ± 0.55	6.40 ± 0.82	0 99	0.87
Sundsvall	0.47 ± 0.07	0.78 ± 0.14	0.69	1.15	0.62 ± 0.13	1.02 ± 0.16	0.81	1.10	2.19 ± 0.29	2.88 ± 0.63	0.96	0.86
Sveg	0.49 ± 0.11	0.81 ± 0.14	0.73	1.18	0.48 ± 0.08	0.64 ± 0.13	0.79	1.13	2.10 ± 0.34	2.56 ± 0.58	1.01	0.90
Umeå	0.39 ± 0.07	0.70 ± 0.11	0.75	1.21	0.47 ± 0.06	0.84 ± 0.15	0.86	1.13	3.11 ± 0.61	3.70 ± 0.74	0.98	0.83
Vänersborg	0.65 ± 0.13	0.94 ± 0.19	0.70	1.13	0.61 ± 0.09	0.70 ± 0.15	0.83	0.96	3.28 ± 0.52	2.98 ± 0.53	1.00	0.74
Vilhelmina	0.37 ± 0.09	0.77 ± 0.19	0.75	1.17	1.08 ± 0.11	0.60 ± 0.11	0.82	1.16	2.22 ± 0.36	2.67 ± 0.53	1.16	0.81
Visby	0.72 ± 0.15	0.62 ± 0.12	0.80	1.07	0.64 ± 0.15	0.68 ± 0.14	0.73	1.16	3.66 ± 0.55	7.57 ± 0.81	0.97	0.96
Mean	0.58 ± 0.11	1.04 ± 0.20	0.76	1.17	0.60 ± 0.11	0.88 ± 0.15	0.80	1.10	2.98 ± 0.49	4.03 ± 0.66	1.04	0.87

[a]The offsets are relative to the 15° solution.

[b]The mean of the absolute values of the offsets. The uncertainty is the standard error of the mean.

[c]Ratio between the mean of the weighted RMS of all baselines to the specific site for the 15° solution and the mean of the weighted RMS of all baselines to the specific site for the 10° or 20° solution.

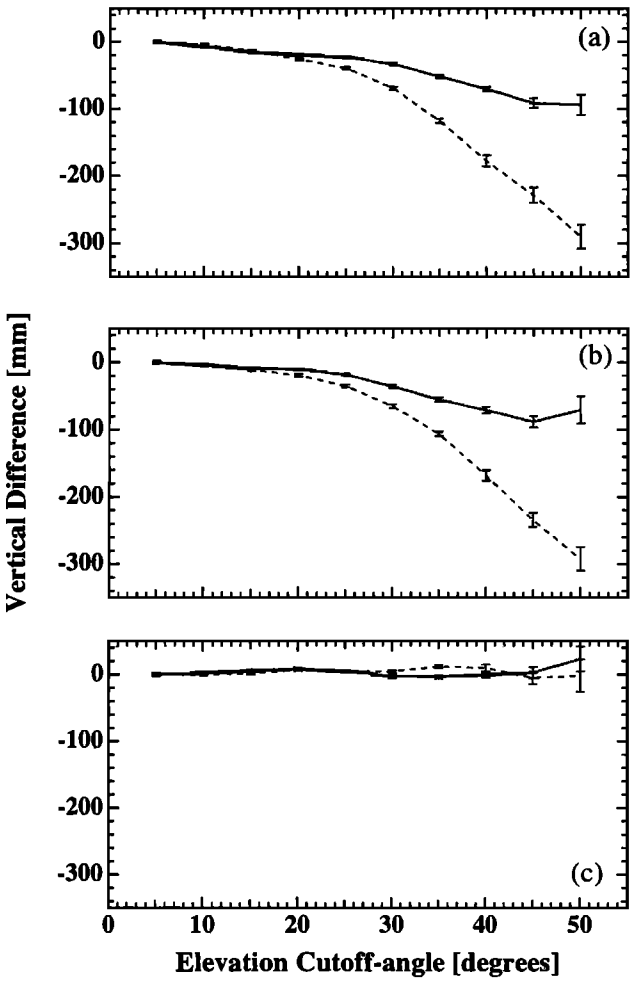

Figure 13. Combined solutions of daily estimates of the vertical component of baseline plotted as a function of elevation cutoff angle for 3 weeks before and 3 weeks after the microwave absorber was employed at the Onsala site. The results are plotted relative to the first 3-week combined solution for a 5° elevation cutoff angle. The baselines are (a) Hässleholm-Onsala, (b) Onsala-Sundsvall, and (c) Hässleholm-Sundsvall. The error bars are the uncertainty of the combined solutions. In Figures 13a and 13b the solid and dashed lines represents results with and without microwave absorber employed at the Onsala site, respectively. In Figure 13c the different lines represent two independent periods.

Kootwijk-Onsala baseline differ by 0.3 ± 1.7 mm between the 15° and 20° solutions in June 1994, and by 9.2 ± 2.0 mm in September 1994, that is, the estimate of the vertical component of baseline from the September data differs by 8.9 ± 2.6 mm from the corresponding estimate from the June data. We attribute this difference to the absorber being in place only during September. We may explain the difference as follows: any scattering effects (or other unmodeled systematic effects) at sites that are used in the transformation to the ITRF will not significantly affect the estimated position of these sites since they are more or less forced (via the weighted least squares process) to a fixed a priori position in the transformation. Any errors in the estimated positions of these sites will therefore instead propagate into the positions of other sites in the network (those that are not involved in the transformation). If the scattering effects are similar at two sites, on the other hand, such as for the Onsala and Kootwijk sites in June 1994, the error will cancel.

Baseline Length Dependence on Estimates of Relative Site Positions

The previous sections mainly investigated absolute values of offsets between solutions obtained for different elevation cutoff angles and to a large degree the mean of these offsets. We have also been concentrating on the effects on baselines formed between sites employed with different pillars and antenna mounts. In this section, we study the sign of the offsets and the dependence of these offsets on the length of the components of the baseline, irrespective of the site monumentation.

Figures 15, 16, and 17 show offsets between estimates obtained for a 15° elevation cutoff angle and estimates

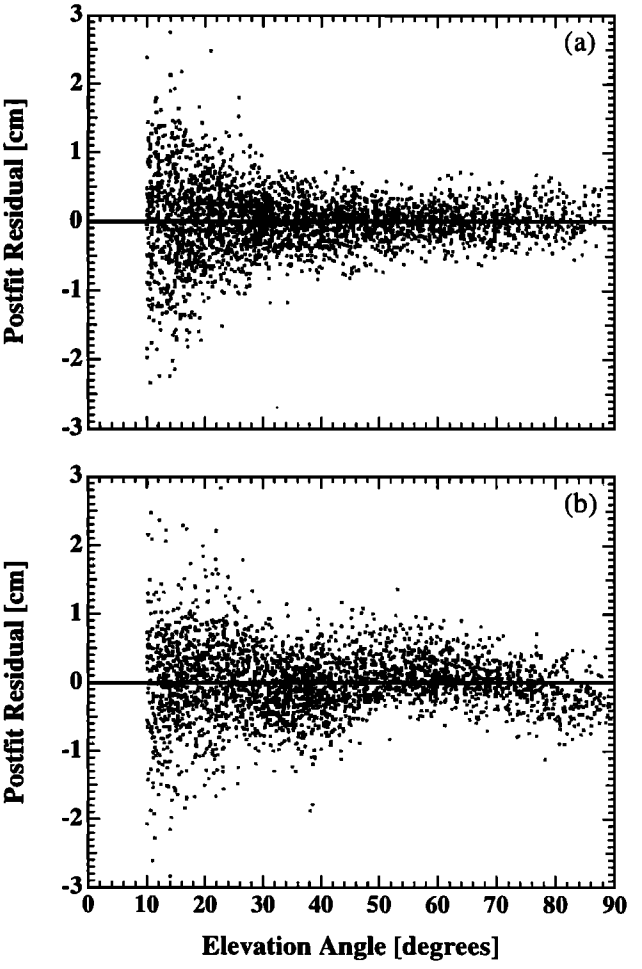

Figure 14. Postfit LC phase residuals for (a) the Hässleholm site and (b) the Kootwijk site for all satellites from the September 16, 1994, data, plotted as a function of elevation angle.

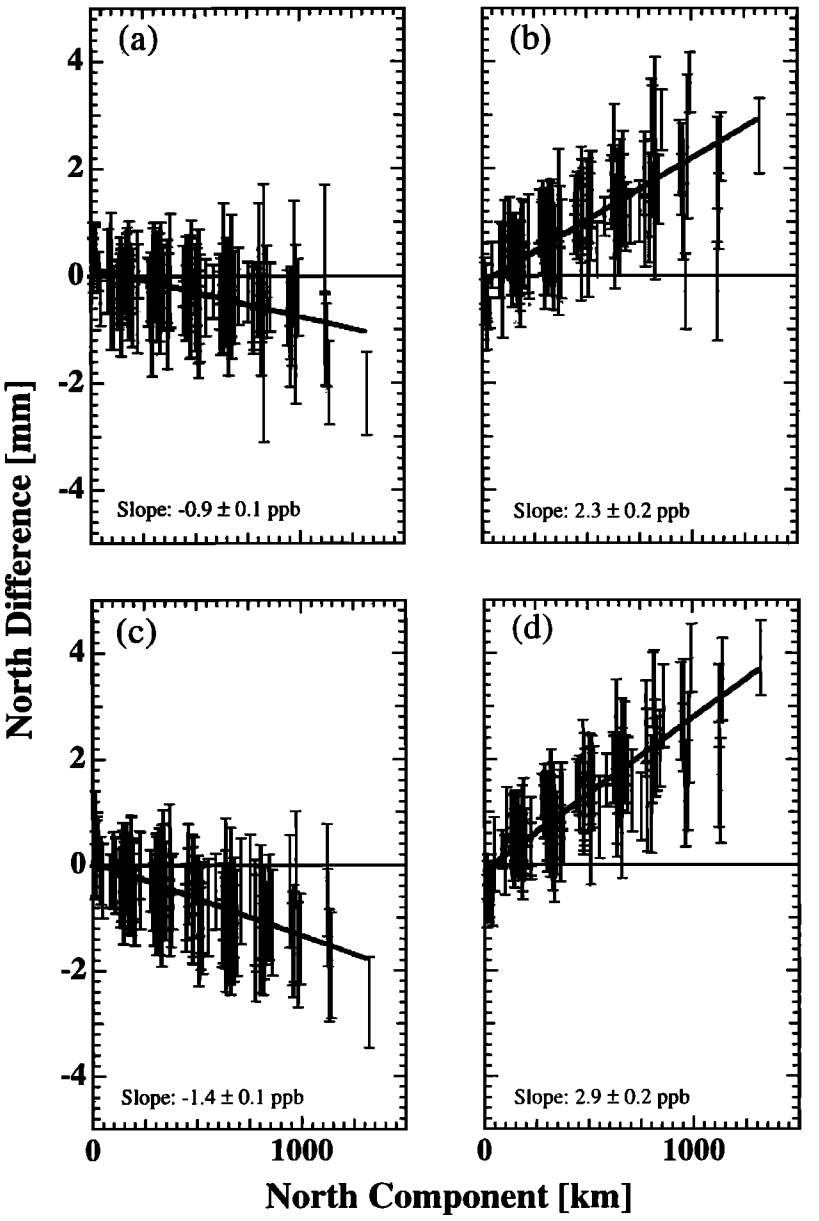

Figure 15. Offsets between monthly combined solutions for different elevation cutoff angles for the north components of all baselines within SWEPOS, plotted as a function of the lengths of the north components. The error bars represent the uncertainty of these offsets. The offsets are between (a) the 15° and 10° solutions in June 1994, (b) the 15° and 20° solutions in June 1994, (c) the 15° and 10° solutions in September 1994, (d) the 15° and 20° solutions in September 1994. The solid line in each plot is the fit of the estimates to a straight line. The slope with its 1-σ uncertainty is given in each plot.

obtained for either 10° or 20° elevation cutoff angle, of the north, east, and vertical components of the baseline. Each point in a plot represents one single baseline within SWEPOS. (Only baselines formed between the 16 SWEPOS sites are included.) The error bars represent the uncertainty of the offsets. A positive offset indicates that the length of the component is decreased. The offsets for the north component (Figure 15), which are plotted as a function of the length of the north component of baseline, reveal a clear component length dependence for both months (June and September 1994), with the dependence being opposite for the 20° solutions compared to the 10° solutions. Similar dependence with component length are also seen in plots of offsets for the east component (Figure 16) even though the dependence is less significant as seen from the uncertainties of the slopes. The offsets for the vertical component (Figure 17), plotted as a function of baseline length, reveal no significant length dependence. The scatter in the June 1994 plots (Figures 17a and 17b) of

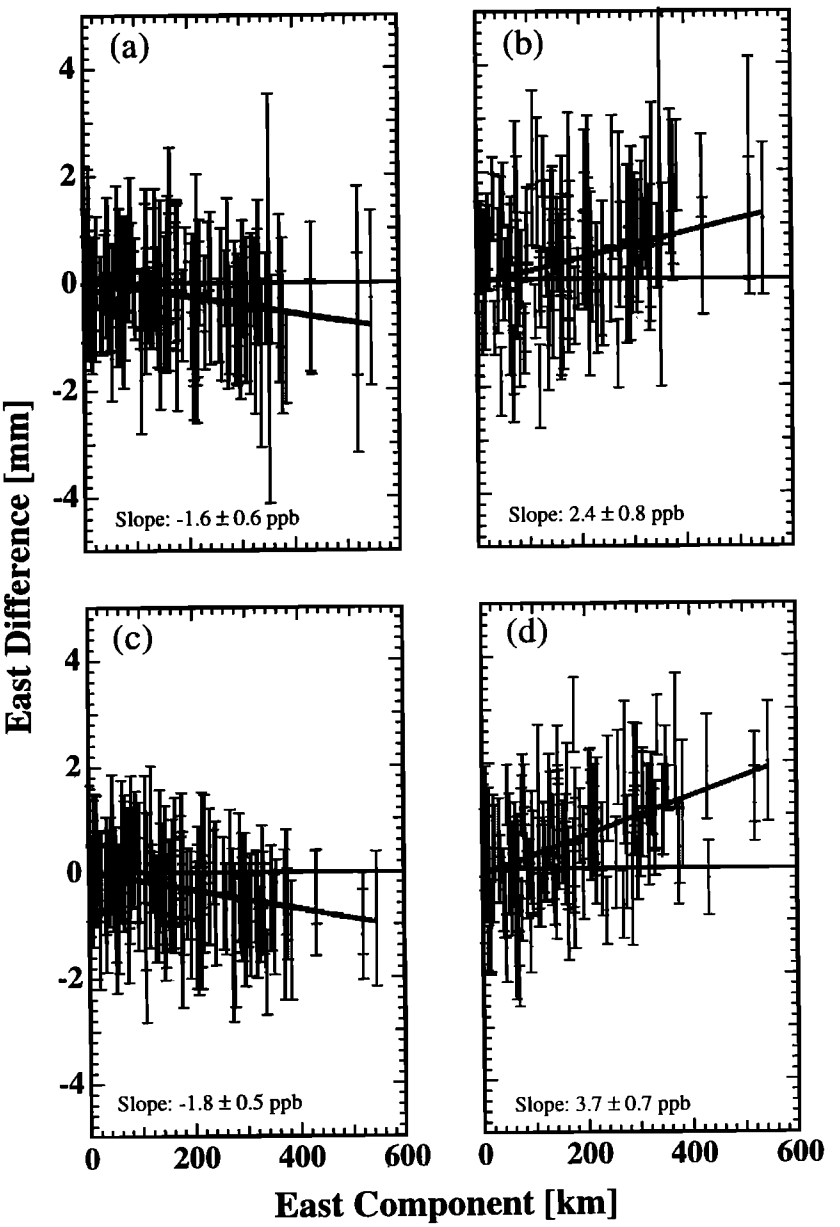

Figure 16. Same as Figure 15, except here for the east component.

the vertical component is larger than for the September 1994 plots (Figures 17c and 17d) mainly because the offsets for the Onsala site are smaller in September.

Figures 18-21 show the offsets for some selected sites. Figure 18 shows offsets for the north component of all baselines to the Hässleholm site. The offsets are plotted as a function of increasing length of the north component and labeled by abbreviated site names. The length dependence is clearly seen. Hässleholm is the most southern site in SWEPOS, and for the longest component lengths, for instance to the Kiruna site, offsets of more than 5 mm are evident between different solutions. Figure 19 shows the offsets in the north component for all baselines to the Sundsvall site. This site is located in the central part of SWEPOS, and baseline lengths to this site are on average shorter, which explains the smaller offsets. Figure 20 and 21 show offsets in the east component for all baselines to the Hässleholm and Kiruna site, respectively. The offsets are plotted as a function of increasing length of the east component. The length dependence in these plots is, especially for the Hässleholm site, less significant.

These results indicate that there are unmodeled systematic effects at all sites of SWEPOS which increase with the length of the horizontal components of baseline. Elevation-angle-dependent variations in antenna phase patterns will be differenced out if two sites observe a satellite with identical elevation angle. For the most southern and most northern sites of SWEPOS, the difference in observed elevation angle for the same satellite can be as much as 10°. Effects from nonuniform antenna phase patterns will therefore not cancel,

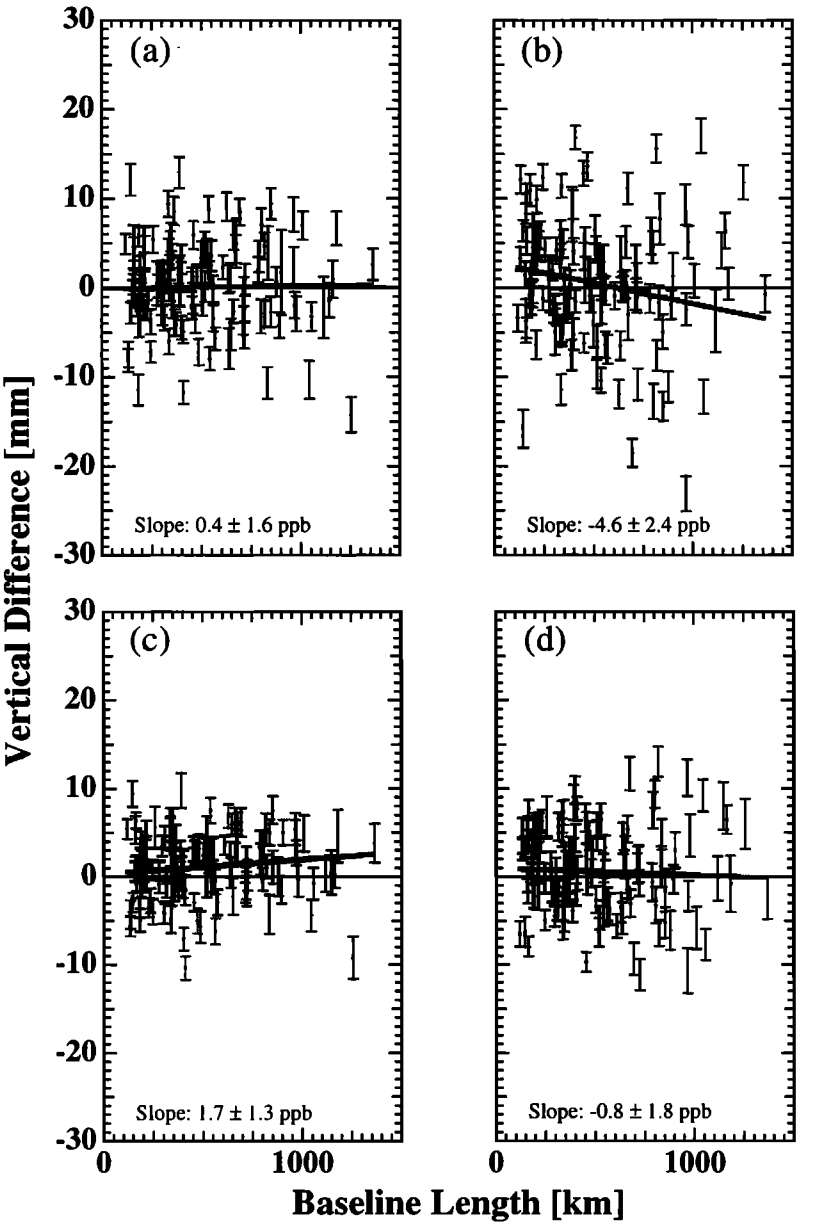

Figure 17. Same as Figure 15, except here for the vertical component, plotted as a function of baseline length.

irrespective of whether or not the phase patterns are identical at sites. This fact might explain the length dependent offsets in the horizontal components of baseline. Scattering effects, identical or not, may also increase this length dependence.

Discussion and Conclusions

We have shown that estimates of relative site positions within the Swedish permanent GPS network (SWEPOS) are affected by scattering from structures associated with the mounting of the GPS antenna to the pillar. The original phase pattern of the identical antennas in the network is distorted individually because of electromagnetic coupling between the antenna and the unique electromagnetic environment at each site. Although we have tried to make the antenna surroundings (pillar and antenna mount) identical at most of the 20 sites of SWEPOS, there is one major exception, namely, the Onsala site.

We found that estimates of the vertical component of baselines to the Onsala site display a systematic dependence on the choice of elevation cutoff angle, an effect similar to what was found for the Westford GPS site in Massachusetts [*Elósegui et al.*, 1995]. The estimated vertical component of the Hässleholm-Onsala baseline changes by 22.3 ± 1.6 mm when the elevation cutoff angle is changed from 10° to 20°. The effect can be significantly reduced by minimizing the scattering from antenna mounting equipment located below the antenna,

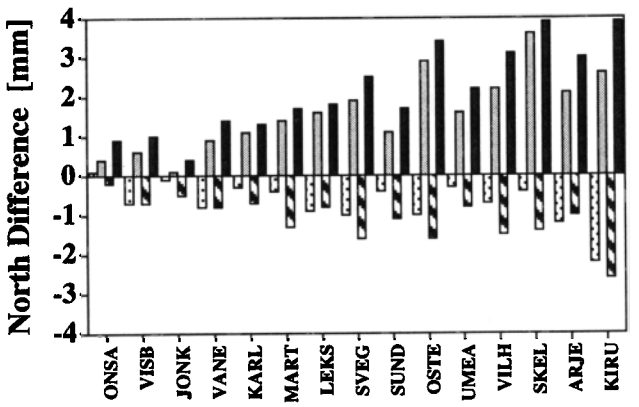

Figure 18. Offsets between monthly combined solutions for different elevation cutoff angles for the north components of all baselines to the Hässleholm site, plotted as a function of increasing length of the north component and labeled by abbreviated site names. The offsets are between (dotted) the 15° and 10° solutions in June 1994, (grey) the 15° and 20° solutions in June 1994, (striped) the 15° and 10° solutions in September 1994, and (solid) the 15° and 20° solutions in September 1994.

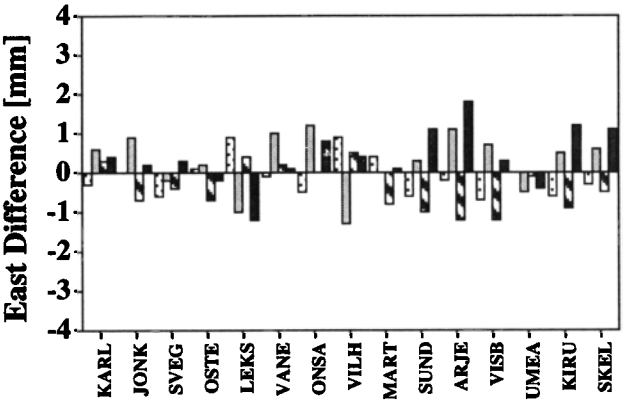

Figure 20. Same as Figure 18, except here for the east component.

for instance, with absorbing material. Remaining scattering may be handled by reducing the side- and backlobe levels of the antenna. An improved antenna design is under investigation, as well as modeling of the scattering effect through a numerical evaluation based on the method of moments. The results of these studies will be reported elsewhere.

We found also that offsets in estimates of the horizontal components of a baseline were not affected by scattering only. In fact, a major part of the unmodeled elevation dependent effects we saw in the horizontal components increased with baseline length, irrespective of the antenna environment. This result indicates that differential phase errors are produced because of nonuniform antenna phase patterns (which might be identical at each site) in combination with the fact that the antennas are "seeing" a certain satellite at different elevation angles.

The results presented in this paper are important for those analyzing data from networks of any size and requiring millimeter-level accuracy in all components. They are also important for those who are intending to set up permanent networks. The success of our own intentions of measuring reliably vertical and horizontal velocities with rates of 0-10 mm/yr are greatly dependent on coping with unmodeled systematic effects at these levels. We do not believe that the pillar system at the Onsala site is much more affected than any other site of the global network. The effects we have seen are due to baselines formed between sites using different types of pillars and antenna mounts. Similar effects are probably also present for sites in the global network, as also indicated in this paper. All users of data from these sites will thus be affected to a level which is not very well documented. Modeling of the scattering effect, or rather the complete phase response of the antenna system, including the pillar, is an important issue for future improvements of the GPS technique. One possibility to minimize these problems would be to agree upon use of one type of antenna/pillar system in the scientific GPS community. This system should, of course, be well-documented and phase-calibrated. As the precision and accuracy of GPS measurements im-

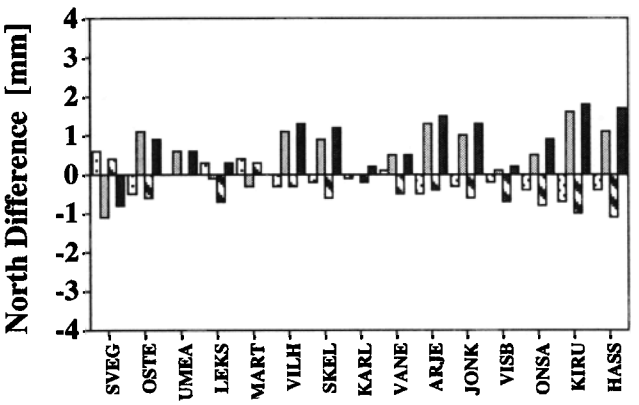

Figure 19. Same as Figure 18, except here for the Sundsvall site.

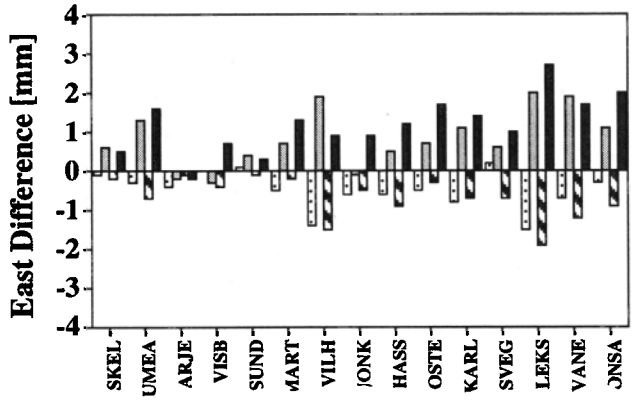

Figure 21. Same as Figure 20, except here for the Kiruna site.

prove in general, antenna phase pattern variations due to different pillars and antenna mounts could be the major error source in just a few years, if not now.

Acknowledgments. We would like to thank the associate editor Robert W. King, referee Thomas A. Herring, and one anonymous referee for their comments and suggestions. Plot routines for production of Figure 1 were kindly provided by *Wessel and Smith* [1995]. This work was supported in part by the Swedish Natural Science Research Council (NFR), the Wallenberg foundation of Sweden, the Smithsonian Institution, and the National Aeronautics and Space Administration (NASA) grants NAG5-538, NAS5-32353, and NAG5-1906.

References

Blewitt, G., Advances in Global Positioning System technology for geodynamics investigations: 1978-1992, in *Contributions of Space Geodesy to Geodynamics: Technology*, Geodyn. Ser., vol. 25, edited by D.E. Smith and D.L. Turcotte, pp. 195-213, AGU, Washington, D.C., 1993.

Blewitt, G., M. Heflin, K. Hurst, D. Jefferson, F. Webb, and J. Zumberge, Absolute far-field displacements from the June 28, 1992, Landers earthquake sequence, *Nature*, *361*, 340–342, 1993.

Bock, Y., et al., Detection of crustal deformation from the Landers earthquake sequence using continuous geodetic measurements, *Nature*, *361*, 337–361, 1993.

Dixon, T.H., An introduction to the global positioning system and some geological applications, *Rev. Geophys.*, *29*, 249–276, 1991.

Dragert, H., and R.D. Hyndman, Continuous GPS monitoring of elastic strain in the northern Cascadia subduction zone, *Geophys. Res. Lett.*, *22*, 755–758, 1995.

Elósegui, P., J.L. Davis, R.T.K. Jaldehag, J.M. Johansson, A.E. Niell, and I.I. Shapiro, Geodesy using the Global Positioning System: The effects of signal scattering on estimates of site position, *J. Geophys. Res.*, *100*, 9921–9934, 1995.

Georgiadou, Y., and A. Kleusberg, On carrier signal multipath effects in relative GPS positioning, *Manuscr. Geod.*, *13*, 172–179, 1988.

Heflin, M., et al., Global geodesy using GPS without fiducial sites, *Geophys. Res. Lett.*, *19*, 131–134, 1992.

Mitrovica, J.X., J.L. Davis, and I.I. Shapiro, A spectral formalism for computing three-dimensional deformations due to surface loads, 2. Present-day glacial isostatic adjustment, *J. Geophys. Res.*, *99*, 7075–7101, 1994.

Schupler, B.R., and T.A. Clark, How different antennas affect the GPS observable, *GPS World*, 32–36, Nov./Dec., 1991.

Schupler, B.R., R.L. Allshouse, and T.A. Clark, Signal characteristics of GPS user antennas, *Navigation*, *41(3)*, 277–295, 1994.

Tranquilla, J.M., Multipath and imaging problems in GPS receiver antennas, paper presented at Fourth International Symposium of Satellite Positioning, DMA, Austin, Tex., 1986.

Tranquilla, J.M., and B.G. Colpitts, GPS antenna design characteristics for high precision applications, paper presented at ASCE Specialty Conference GPS-88: Engineering Applications of GPS Satellite Surveying Technology, Am. Soc. Civ. Eng., Nashville, Tenn., May 11–14, 1988.

Tranquilla, J.M., J.P. Carr, and H.M. Al-Rizzo, Analysis of a choke ring groundplane for multipath control in Global Positioning System (GPS) applications, *IEEE Trans. Antennas Propag.*, *42*, 905–911, 1994.

Tsuji, H., Y. Hatanaka, T. Sagiya, and M. Hashimoto, Coseismic crustal deformation from the 1994 Hokkaido-Toho-Oki earthquake monitored by a nationwide continuous array in Japan, *Geophys. Res. Lett.*, *22*, 1669–1672, 1995.

Young, L.E., R.E. Neilan, and F.R. Bletzacker, GPS satellite multipath: An experimental investigation, paper presented at First International Symposium on Precise Positioning With the GPS, NOAA, Rockville, Md., 1985.

Webb, F.H., and J.F. Zumberge, An introduction to the GIPSY/OASIS-II, *JPL Publ.*, *D-11088*, 1993.

Wessel, P., and W.H.F. Smith, New version of the Generic Mapping Tools released, *Eos Trans. AGU*, *76*, 329, 1995.

J. L. Davis and I. I. Shapiro, Harvard-Smithsonian Center for Astrophysics, 60 Garden Street, Cambridge, MA 02138. (e-mail: jdavis@cfa.harvard.edu; shapiro@cfa.harvard.edu)

P. Elósegui, ESA-INSA, IUE Observatory, VILSPA Satellite Tracking Station, Apartado - P.O. Box 50727, E-28080 Madrid, Spain. (e-mail: pel@vilspa.esa.es)

R. T. K. Jaldehag, Swedish National Testing and Research Institute, Box 857, S-50115, Borås, Sweden. (e-mail: kenneth.jaldehag@sp.se; rkj@oso.chalmers.se)

J. M. Johansson and B. O. Rönnäng, Onsala Space Observatory, Chalmers University of Technology, Department of Radio and Space Science, S-43992 Onsala, Sweden. (e-mail: jmj@oso.chalmers.se; bor@oso.chalmers.se)

A. E. Niell, Haystack Observatory, Westford, MA 01886. (e-mail: aen@bashful.haystach.edu)

(Received September 27, 1995; revised April 1, 1996; accepted April 9, 1996.)